論文
Paper

Experimental Study on Transient Boiling Heat Transfer and Critical Heat Flux on Horizontal Vertically-Oriented Ribbon with Different Surfaces under Atmospheric Conditions*

Min Han Htet*1 Katsuya FUKUDA*2 Qiusheng LIU*2

A deep understanding of transient pool boiling heat transfer and critical heat flux (CHF) phenomena in water is important as a fundamental knowledge for the innovative design of liquid cooling technologies. Transient CHF due to exponentially increasing heat inputs, $Q=Q_0\exp(t/\tau)$, to platinum ribbon in pool of water was measured for saturated conditions at atmospheric pressure. The exponential period, τ, was varied from 5 ms to 20 s. The platinum ribbons having different surface conditions, namely, commercial surface (CS), treated surface-I (TS-I) and treated surface-II (TS-II) were utilized as test heaters. For surface conditions, the values of contact angle and surface roughness were measured prior to pool boiling experiments. The TS-II was subjected to conditions without pre-pressurization and with pre-pressurization up to 4.4 MPa before each experimental run was carried out. It is assumed that the contact angle is a major contributor to increasing CHF at quasi-steadily heat input. The TS-II enhanced the heat transfer performance ~ 290 % and ~ 430 %, and CHF of 1.2 times and 1.5 times relative to CS and TS-I, respectively. It was shown that transition of heat transfer processes and transient CHF depend on surface conditions, heat generation period and pre-pressurization. The transient CHF due to surface conditions was compared with corresponding values.

1. Introduction

Modification of cooling system to enhance the critical heat flux (CHF) is important for many engineering applications including nuclear fuel rods, water-cooled trunbine blades, supercomputers, marine engine system and so on [1,2]. CHF was considered to be due to hydrodynamic instability (HI) [3,4]. However, CHF was influenced not only HI but also heterogeneous spontaneous nucleation (HSN) and the occurrence of HSN depends on surface condition [5,6]. In this aspect,the deep understanding of the transient pool boiling heat transfer and critical heat flux (CHF) with surface condition is becoming important to improved design of liquid cooling technologies [5,6]. Various techniques of surface enhancement were applied which included making re-entrance type cavities to control cavity geometry, deposition of porous/ non-porous layer to get desired porousity and roughening a surface using smooth or rough paper [6-8]. Moreover, wettability which have relationship on roughness, porousity and liquid properties is one of important factors of surface condition can be determined by contact angle [8]. Various researchers discussed the nucleate boiling heat transfer and CHF in consideration to maximize CHF. The cavity-mouth diameter determines surface superheat needed and contact angle is vital at bubble nucleation primarily [9]. The effects of the interface-variables due to surface roughness and contact angle have found at the heat transfer surface on nucleate boiling [10]. However, CHF was independent of modified surface condition [11]. Alternatively, CHF test using horizontal vertically oriented steel ribbon heaters under saturated pool boiling in FC-72 at atmospheric pressure revealed that surface roughness can increase CHF by 6 ~ 12% [12]. The CHF correlation which contains both surface roughness and contact angle on flat heaters was postulated taking account the influence of surface roughness [13]. In addition, porousity have strongly affected on CHF according to the separated tests with contact angle, porosity and roughness [8].

*Received May 9, 2015
*1: Graduate School of Maritime Sciences, Kobe University
*2: Marine Engineering Division, Kobe University

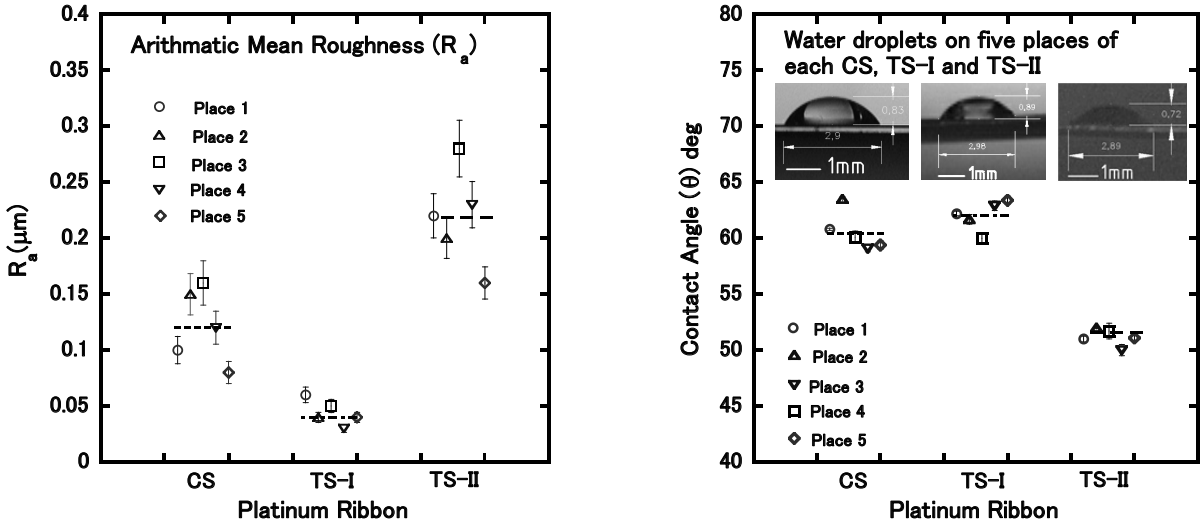

(a) (b)

Fig. 1 The results of (a) surface roughness and (b) contact angle for CS,TS-I and TS-II

Transient CHF due to exponential increasing heat inputs on horizontal cylinders with different surface roughnesses in pool of water using without and with pre-pressurization before each experimental run have stated that a heat transfer crisis, namely, heterogeneous spontaneous nucleation (HSN), was observed due to direct transition from natural convection to film boiling without nucleate boiling [5,6]. It was occurred that the physical mechanism of CHF due to HSN contradicts from classical hydrodynamic instability theory. Besides, the pre-pressurization can make contact angle hysteresis at highly subcooled conditions prior to a transient and nucleate boiling was significantly suppressed [14]. The investigation on rough surface ascertained that it can increase CHF at transient heat transfer process by improving surface energy.

Furthermore, heterogeneous nucleate boiling was investigated on ultra-smooth surfaces with root mean square (RMS) roughness of 0.03−0.365 μm for brass, unpolished stainless steel, and electropolished stainless steel in pentane and butane at steady boiling condition [15]. Surface orientation is important factor that can greatly degrade the CHF. The upward-facing surface has maximum CHF, conversely, downward- facing has minimum one due to difficult bubble detachment [16]. In this regard, the bubble departure rate increases with the decreasing value of contact angle [17]. The combined effect of surface orientation and contact angle at various surface roughnesses of flat plate heaters is also well-known correlation [18].

The present study clarifies the transient heat transfer and CHF on the multi-effects of surface roughness, contact angle, heat generation period, and pre-pressurization on horizontal vertically-oriented ribbon heaters. For surface condition, commercial surface (CS), treated surface I (TS-I) and treated surface II (TS-II) were prepared. For the TS-II, the two pre-pressurization cases, without and with pre- pressurization up to 4.4 MPa, namely, TS-II (0/4.4 MPa), respectively, were carried out before each experimental run. Experiments are conducted under saturated condition at atmospheric pressure in pool of water.

2. Experimental Apparatus and Method

2.1 Treatment of Test Heater

The heater dimension of width, thickness and effective length for the CS, TS-I and TS-II are $(4\times0.1\times30)$ mm, $(4\times0.1\times30)$ mm and $(4\times0.2\times41)$ mm, respectively. The TS-I and TS-II were treated from commercially available ribbon. The former was polished with buff paper and alumina suspension. The latter was finished by emery paper with granularity of #1500. The surface roughnesses of each heater were measured by a profilometer, Handysurf- E-35-A. The heaters were cleaned with acetone. To measure the contact angle, ion-exchange-water droplets with an amount of 4 μm each after distillation were dropped onto the one of the surfaces with the aid of the autoclavable

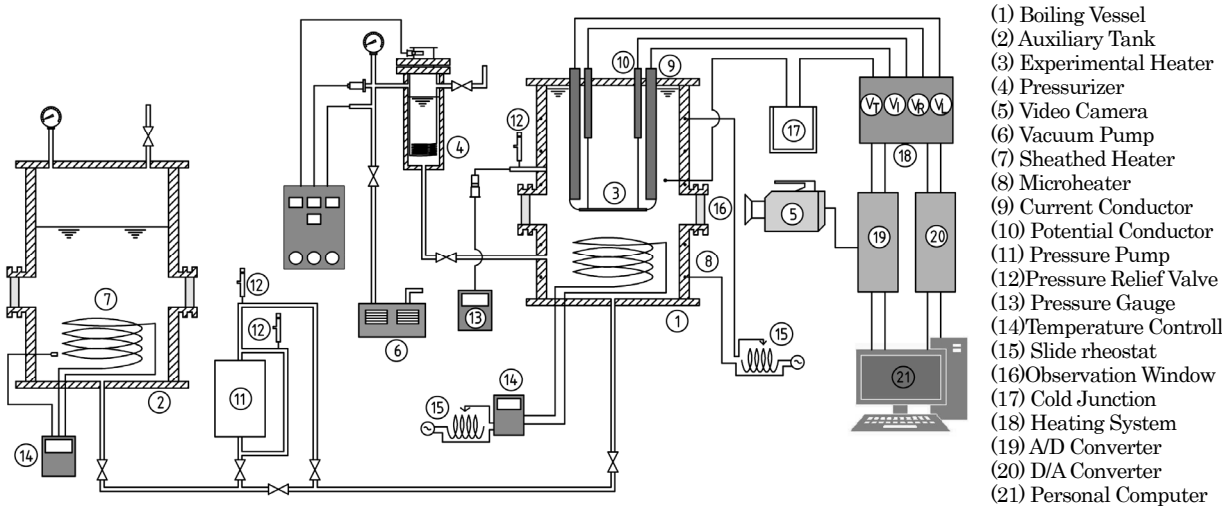

Fig. 2 Experimental Pool boiling apparatus

pipettor (0.5-10 μl). The image of the droplet was attained by CCD camera and Ulead-image-capturing software which was installed in computer. The actual dimensions of each droplet were measured by AutoCAD software. The contact angle, θ, was calculated with the equation suggested by Honjo, et al. [19].

The results of surface roughness and contact angle measured on the CS, TS-I and TS-II are shown in Fig. 1 (a) and (b). The surface roughness value at the vertical axis of Fig. 1 (a) shows the arithmetic mean roughness, R_a. The average values of R_a for the CS, TS-I and TS-II are 0.12 ± 0.015μm, 0.04 ± 0.005 μm and 0.22 ± 0.02 μm, respectively. Moreover, the average values of θ are 60.6 ±1.3º, 62.0 ± 1.0º and 51.5 ± 0.7º, respectively. It can be seen that the largest value of R_a with respect to the TS-II value yields the smallest value of θ and the smallest value of R_a related to the TS-I reveals the largest value of θ. It is compromise with the relation between surface roughness and contact angle for copper and stainless steel [20] in which the values of contact angle decrease from maximum value to minimum one with an increase of surface roughness from lowest value up to 0.25 μm. It was desirable that the surface with large roughness and small contact angle decrease the ΔT_i due to HSN and increase CHF.

2.2 Experimental Pool Boiling Apparatus

The experimental pool boiling apparatus is shown in Fig. 2. It is mainly comprised of a boiling vessel (1), a test section including horizontal vertically oriented platinum ribbon heater (3), a pressurizer (4), a pressure pump (11), heating system (18), and a data measurement and processing system (19)-(21), and a video camera system (5). The boiling vessel is made of cylindrical stainless steel with 20-cm inner diameter and 60-cm height capable of operating up to 5 MPa. The two current conductors and two potential conductors were installed at the upper side of the vessel, which were also used to support the test heater. Two fine 30 μm diameter platinum wires (potential taps) are spot-welded on the heater at about 10 mm from each end of the heater. The effective length of the heater between the potential taps was about 30 mm for CS and TS-I, and 41 mm for TS-II. The vessel is equipped with a pressure transducer and a sheathed 1 mm diameter K-thermocouple to measure the bulk liquid temperature.

2.3 Experimental Method and Procedure

The test heater was calibrated at various liquid temperatures using double bridge circuit to attain the resistance-temperature relation, $R_T = R_0\ (1 + \alpha T + \beta T^2)$, where, $R_T(\Omega)$ is resistance in a double bridge circuit, and α and β are fitted constant. The value of β is -5.88×10^{-7} for Grade 1 annealed platinum at temperatures up to 1500ºC [21]. Then, the test heater including the test section was mounted to the current and potential conductors of the boiling vessel. The test heater as a branch of a double bridge circuit was balanced at the bulk liquid temperature.

The heat input signal was transmitted to electronic switch from a digital computer through a digital-to-analog (D/A) converter. For desired time

function for the heat input, controllable D.C. electric power (800A, 15V) [22] was supplied to test heater. The voltage drops across a standard resistance, across the potential taps of the heater and the output voltages of the double bridge circuit were passed to computer via amplifiers and analog-to-digital (A/D) converter. They were simultaneously monitored at a constant time interval ranging from 60 μs ~120 ms to evaluate heat generation rate, Q , and average temperature, T_a .

Average temperature, T_a , is calculated according to the previous resistance-temperature relation. If the value of T_a is higher than shut off temperature which have already set up in computer, the power shut off signal will be sent to electronic switch to cut out the power supply not to occur actual burnout of the heater.

The heat generation rate of the heater, Q , was determined by the multiplication of the current to heater and the voltage difference between potential taps of the heater. As heat generation rate will change simultaneously with resistance change of test heater, a heat generation control system have developed using a high-speed analog computer [23].

The heat flux, q , of the heater during experiment is computed by the difference between the heat generation rate per unit surface area, Q, and the rate of change of energy storage in the heater as follows:

$$q = \frac{\delta}{2}\left[Q - \rho_h c_h \frac{dT_a}{dt} \right] \tag{1}$$

where, ρ_h , c_h and δ are the density, the specific heat and the half thickness of heater, respectively.

The surface temperature, T_s, was calculated by the following unsteady heat conduction equation of heater.

$$\left.\frac{\partial T}{\partial t}\right| = a\frac{\partial^2 T}{\partial x^2} + \frac{Q}{\rho_h c_h} \tag{2}$$

Boundary conditions are as follows:

$$\left.\frac{\partial T}{\partial x}\right|_{x=0} = 0, \quad k\left.\frac{\partial T}{\partial x}\right|_{x=\delta/2} = q \tag{3}$$

$$T_a = \frac{\int_0^{\delta/2} T dx}{\int_0^{\delta/2} dx} = \frac{2}{\delta}\int_0^{\delta/2} T dx \tag{4}$$

where, a in Eq. (2) and k in Eq.(3) are thermal diffusivity and thermal conductivity, respectively.

The uncertainties were estimated to be about ±1K in the heater surface temperature and ±2 % in the heat flux.

Ion-exchange-distilled water was fully filled in the boiling vessel with the free surface only in the pressurizer and auxiliary tank. Then, the liquid in each tank is separately heated by sheathed heaters installed in each tank. Every tank was degassed by keeping it boiling for 30 minutes at least. The vessel was kept warm by micro heater and lagging materials. Pre-pressurization to the boiling vessel was carried out with a reciprocating diaphragm pump before each experimental run.

The exponential function, $Q = Q_0 \exp(t/\tau)$,where, t means time and τ means exponential period, was set up for heat input. The CHF was determined at a start point where the average temperature rapidly increases up to the preset temperature by using a burnout detector.

3. Experimental Results and Discussion

3.1 Experimental Conditions

The experimental conditions for CS, TS-I and TS-II to perform transient CHF due to exponential increasing heat inputs in this study are described in Table 1.

Table 1. Experimental conditions

Parameter	CS	TS-I	TS-II
Liquid	Water	Water	Water
Q(Heat input)	$Q_0\exp(t/\tau)$	$Q_0\exp(t/\tau)$	$Q_0\exp(t/\tau)$
P(System Pressure)	101.3 kPa	101.3 kPa	101.3 kPa
ΔT_{sub} (Subcooling)	0 K	0 K	0 K
τ (Period)	5 ms ~ 5 s	5 ms~ 20 s	7 ms ~ 20 s
Pressurization	0 MPa	0 MPa	0/4.4 MPa
Material	Platinum	Platinum	Platinum
L(length)	30 mm	30 mm	41 mm
W(Width)	4 mm	4 mm	4 mm
$2\times\delta$ (Thickness)	0.1 mm	0.1 mm	0.2 mm
R_a	0.12 ± 0.015μm	0.04 ± 0.005μm	0.22 ± 0.02 μm
θ	60.6± 1.3°	62.0± 1.0°	51.5± 0.7°

3.2 Effect of Pre-pressurization to Surface Superheat at Boiling Initiation

The results of surface superheat at boiling initiation, ΔT_i, due to quasi-steadily increasing heat inputs versus pre-pressurization are shown in Fig.3. Pre-pressurization up to 4.4 MPa before each experimental run was carried out on horizontal vertically oriented ribbon heater with the TS-II having R_a value of 0.22 ± 0.02 μm and θ value of 51.5 ± 0.7° in water under saturated condition at atmospheric pressure. The pre-pressurization can change active cavities to flooded cavities. In this experiment, the ΔT_i due to quasi-steadily increasing heat inputs and inducing of heterogeneous spontaneous nucleate boiling were investigated. The two demonstrated straight lines based on the measured results revealed that they have different mechanisms at boiling initiation. The line represented for the increasing ΔT_i value up to pre-pressurization of 0.88 MPa is suggested to be due to nucleation sites on the surface of ribbon heater. On the contrary, the ΔT_i values which are approximately constant for pre-pressurization from 0.88 to 4.4 MPa at 20 K are assumed to be due to HSN. The limit of ΔT_i which is about 40 K due to HSN on horizontal cylinder for quasi-steadily increasing heat input in pool of water by pre-pressurization up to 5 MPa have been reported by Sakurai [5]. As the ΔT_i due to HSN depends on surface condition, the value of ΔT_i due to HSN in this study by pre-pressurization up to 4.4 MPa to the TS-II is lower than the ΔT_i due to HSN attained on commercially available horizontal cylinder.

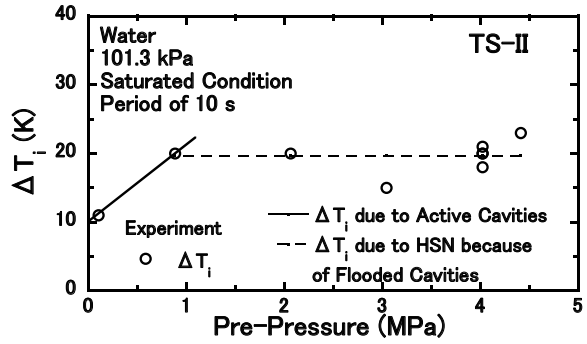

Fig. 3 Surface superheat at boiling initiation vs. pre-pressurization

3.3 Effect of Pre-pressurization to Time Dependence of Surface Temperature, Heat Flux and Heat Generation Rate

The time dependence of surface temperature, T_s, heat flux, q, and Heat Generation Rate, Q, versus pre-pressurization is shown in Fig. 4. They were performed due to exponential heat input for the period, τ, of 500 ms on TS-II (4.4 MPa) in a pool of boiling water at 101.3 kPa. The heat generation rate, Q, increases exponentially for the whole process. However, T_s and incipient heat flux, q_i, increase along heat generation curve up to overshot temperature at boiling initiation, T_{ov}, and q_i, respectively. Then, they decreases rapidly and again increases gradually up to the CHF point. It is suggested that the phenomena such as T_{ov} and delayed q_i are due to the pre-pressurization up to 4.4 MPa which is able to flood the test heater.

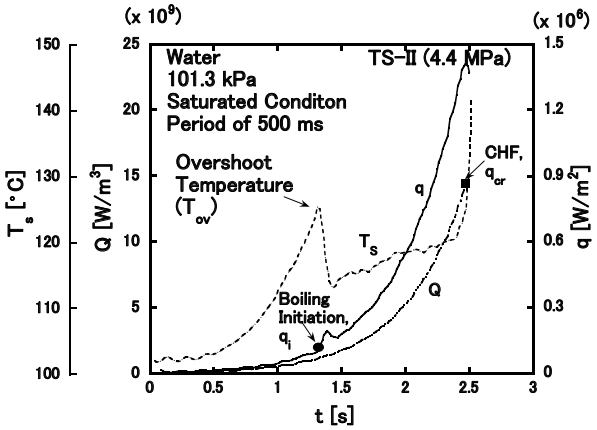

Fig. 4 Time dependence of heat generation rate, surface temperature and heat flux for TS-II (4.4 MPa)

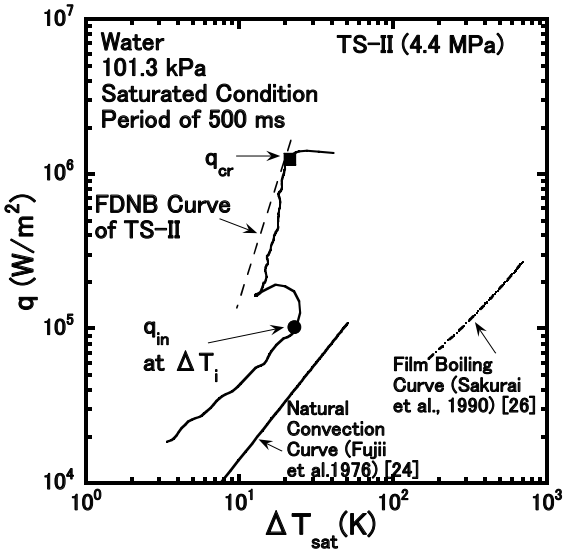

Fig.5 The heat transfer process for TS-II (4.4 MPa) which is depicted in Fig.4

The heat transfer process, q, in Fig. 4 is depicted in Fig.5 as the function of surface superheat, $\Delta T_{sat} = T_s - T_{sat}$. The T_{sat} is saturated temperature of liquid. In this figure, the heat transfer process increases from natural convection to film boiling through fully developed nucleate boiling (FDNB). Decreasing of ΔT_{sat} after boiling initiation, ΔT_i, is due to activation of flooded cavities. The natural convection curve [24], fully developed nucleation curve [25] and steady-state film boiling curve [26] are illustrated for comparison.

3.4 Physical Mechanism of Boiling Heat Transfer due to Pre-pressurization and Exponential Increasing Heat Inputs

The heat flux, q, is characterized by the relation of heat transfer coefficient, h, and ΔT_{sat} as follow:

$$q = h\Delta T_{sat} \tag{5}$$

In boiling heat transfer, q is divided into two conditions such as non-boiling and nucleation condition. Consequently, h can be categorized as non-boiling heat transfer coefficient and nucleate heat transfer coefficient. Non-boiling heat transfer coefficients due to exponential increasing heat inputs governed by natural convection heat transfer, transient conduction heat transfer and combined natural convection and transient conduction heat transfer [22] play role the different physical mechanisms of CHF. Generally, the transient conduction at non-boiling condition due to exponential increasing heat inputs is a major potential model to outcome CHF at q_i. Moreover, it is assumed that dissipation of nucleation sites due to surface condition and pre-pressurization can change the transition of heat flux. It is important to know what factor influences the mechanistic model at non-boiling and nucleation condition which shapes the CHF.

The heat flux at nucleate boiling, q_{nb} and q_i at boiling initiation can be characterized in Eqs. (6) and (7) [25] as follows:

$$q_{nb} = C_1 \Delta T_{sat}^n \tag{6}$$

$$q_i = C_2 \Delta T_i^n \tag{7}$$

where, the value of n in superscripts of Eqs. (6) and (7) is taken as 3.0 by [25]. The subscripts nb, i, C_1 and C_2 mean nucleate boiling, boiling initiation, factors of q_{nb} and q_i, respectively. As the ΔT_{sat} in Eq. (5) is inserted into Eqs. (6) and (7), factors of heat fluxes in Eqs. (8) and (9) were obtained.

$$C_1^{1/n} = h / q^{(n-1)/n} \tag{8}$$

$$C_2^{1/n} = h / q_i^{(n-1)/n} \tag{9}$$

The factors of heat flux depending of time due to heat inputs for period, τ, of 9 s, 100 ms and 20 ms were illustrated with the function of non-dimensional period, (t/τ) in Fig.6. The higher increasing rate of heat input results from the shorter exponential period. It can be seen that the higher increasing rates of heat inputs have higher values of (t/τ). All factors of heat fluxes descending from higher value down to lower one at boiling initiation terminates at the same line representing for $C_2^{1/n}$. On the contrary, at (t/τ) < 4, heat transfer value increase again after boiling initiation. In this case, the lower value of (t/τ) resulting from exponential period, τ, of 9 s reaches to $C_1^{1/n}$. However, at (t/τ) > 4, heat transfer value rapidly decreases after boiling initiation.

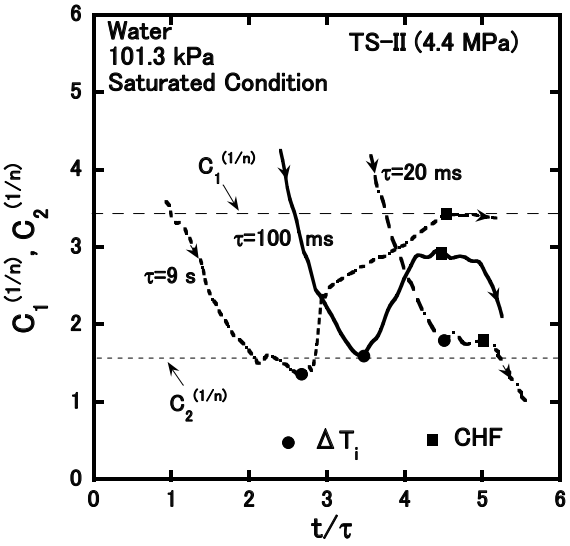

Fig. 6 Boiling heat transfer mechanism due to pre-pressurization and exponential increasing heat inputs

3.5 Typical Heat Transfer Processes of Transient CHF

Fig. 7 illustrates the heat transfer processes due to quasi-steadily exponential heat input for CS (0 MPa), TS-I (0 MPa) and TS-II (0/4.4 MPa). The transition of the heat transfer processes increases from natural convection regime to film boiling

through fully developed nucleated boiling (FDNB). The boiling initiation commences at natural convection regime.

The surface superheat at boiling initiations, ΔT_i, which is shown by solid circles are 9 K, 21 K and 23 K and 25 K with respect to the TS-II (0 MPa), CS (0 MPa), TS-II (4.4 MPa) and TS-I (0 MPa), respectively. It was occurred that the values of the ΔT_i depend on surface condition and the ΔT_i for the TS-I (0 MPa) is higher than the ΔT_i due to HSN obtained by TS-II (4.4 MPa) which is shown in Fig.7. For the TS-II (4.4 MPa), the surface superheat, ΔT_{sat}, decreases due to activation of flooded cavities after boiling initiation. In nucleate boiling regime, the heat transfer processes of the TS-II (0 MPa) and the TS-II (4.4 MPa) become identical regardless of the pre-pressurization. The TS-II (0/4.4 MPa) enhance the boiling heat transfer at the nucleate boiling regimes though the TS-I (0 MPa) reveals degradation of boiling heat transfer in this regime. As the surface superheat, ΔT_{sat}, at the nucleate boiling regimes for TS-II (0/4.4 MPa) decrease 7 K and 10 K, when compared with those of CS (0 MPa) and TS-I (0 MPa), respectively, it can be calculated by using the Eqs.(6) and (8) that the enhancement of the boiling heat transfer at the nucleate boiling regimes due to the TS-II (0/4.4 MPa) is ~ 290% and ~ 430 % when compared with those of CS (0 MPa) and TS-I (0 MPa), respectively.

The heat transfer processes at the FDNB regimes for the TS-II (0/4.4 MPa), the CS (0 MPa) and TS-I (0MPa) were compared with Rohsenow's correlation [25]. The FDNB curves of the TS-II (0/4.4 MPa), the CS (0 MPa) and the TS-I (0 MPa) according to the Rosehnow's correlation are illustrated by broken lines in Fig. 7. The Rohsenow's correlation is as follow:

$$q = \mu_l h_{lv}\left[\frac{g(\rho_l - \rho_v)}{\sigma}\right]^{1/2}\left(\frac{c_{pl}\Delta T_{sat}}{C_{sf} h_{lv} Pr_l^n}\right)^3 \quad (10)$$

where, the values of the liquid-solid combination, C_{sf} , for water-platinum in Eq. (10) was taken as 0.013 and the exponent, n, of Prandtl number for water, Pr_l , was 1.7 [25]. The heat transfer process of the TS-II (0/4.4 MPa) in this study compromises the Rohsenow's correlation with C_{sf} =0.013. However,

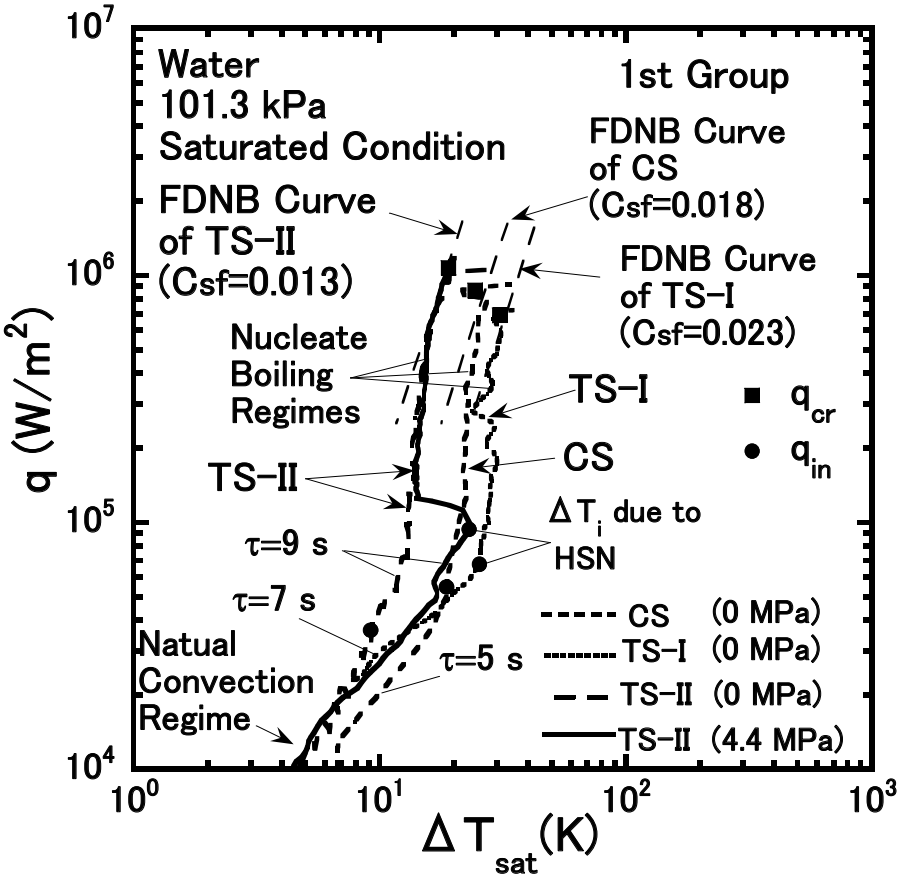

Fig.7 Typical heat transfer processes from natural convection to film boiling through FDNB

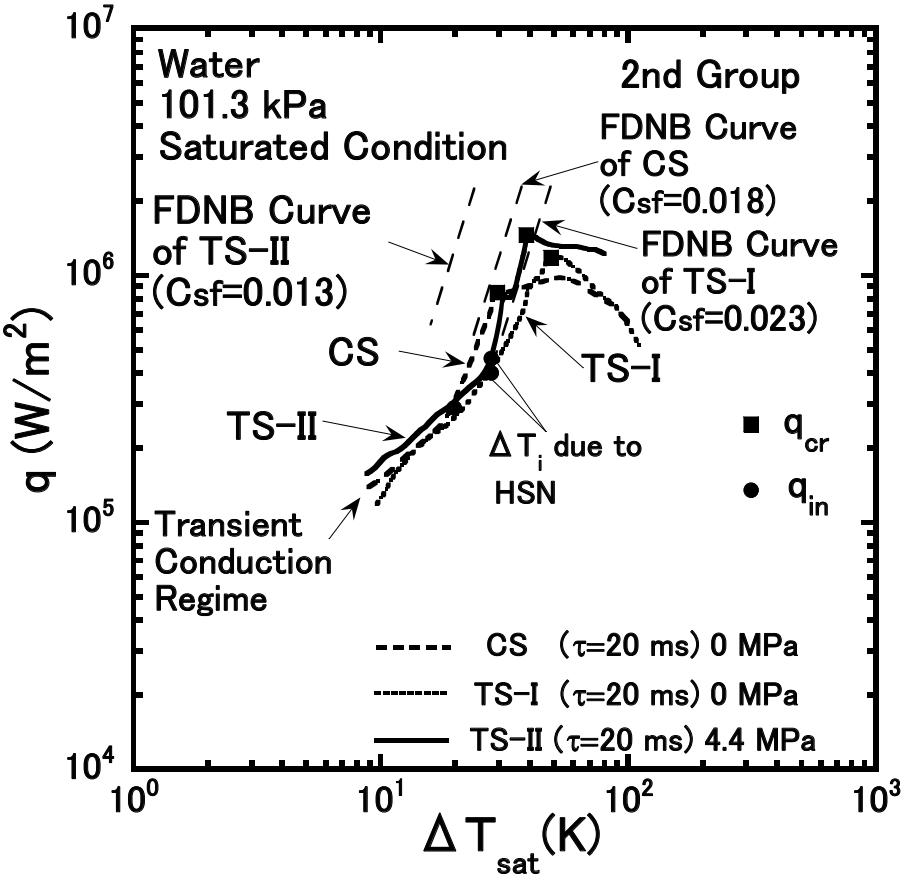

Fig.8 Typical heat transfer processes from transient conduction to film boiling with a nucleate boiling for a while

C_{sf} =0.018 and C_{sf} =0.023 are found at the heat transfer processes of the CS (0 MPa) and TS-I (0 MPa), respectively.

The values CHFs for the TS-II (0/4.4 MPa), the CS (0 MPa) and the TS-I (0 MPa) are 1.14 MW/m², 0.95 MW/m² and 0.76 MW/m², respectively, which are depending on the surface condition. The better contribution of CHF due to the TS-II (0/4.4 MPa) would be due to enhanced surface condition, especially, having small contact angle of the TS-II could generate a higher rate of vapor departure. As is seen in the Fig.7, the surface superheat at the CHF for the TS-II (0/4.4 MPa) is lower than the ΔT_i due to HSN attained on TS-II (4.4 MPa). These kinds of heat transfer processes are generally found at the longer period or τ >100 ms though it is depending on the surface condition.

The heat transfer process due to exponential period, τ , of 20 ms for CS (0 MPa), TS-I (0 MPa) and TS-II (0/4.4 MPa) is shown in Fig.8. The heat transfer processes increases from transient conduction to film boiling with a nucleate boiling for a while. The heat transfer processes initiate their boiling on conduction regime, respectively. The ΔT_i indicated by solid circles are found at 19 K and 29 K and 29 K for the CS (0 MPa), the TS-II (4.4 MPa) and the TS-I (0 MPa), respectively. The ΔT_i for the TS-II (4.4 MPa) and the TS-I (0 MPa) are higher than the ΔT_i due to HSN obtained by TS-II which is shown in Fig.3. After boiling initiation, the heat transfer processes instantly increase to CHFs with a slight increase of surface superheat, ΔT_{sat}, without passing FDNB regimes which are plotted by broken lines in Fig.8. It is due to the fact that the occurrence of the ΔT_i due to HSN which is, then, followed by rapid increasing heat inputs can degrade the heat transfer and reach to the CHFs in shortly. Moreover, it can be seen that the heat transfer process due to pre-pressurization of 4.4 MPa, TS-II (4.4 MPa), has the same transition with the TS-I (0 MPa) and the CS (0 MPa) from non-boiling to film boiling though the TS-II has the large surface roughness, R_a , and small contact angle, θ. After CHFs, the heat transfer processes

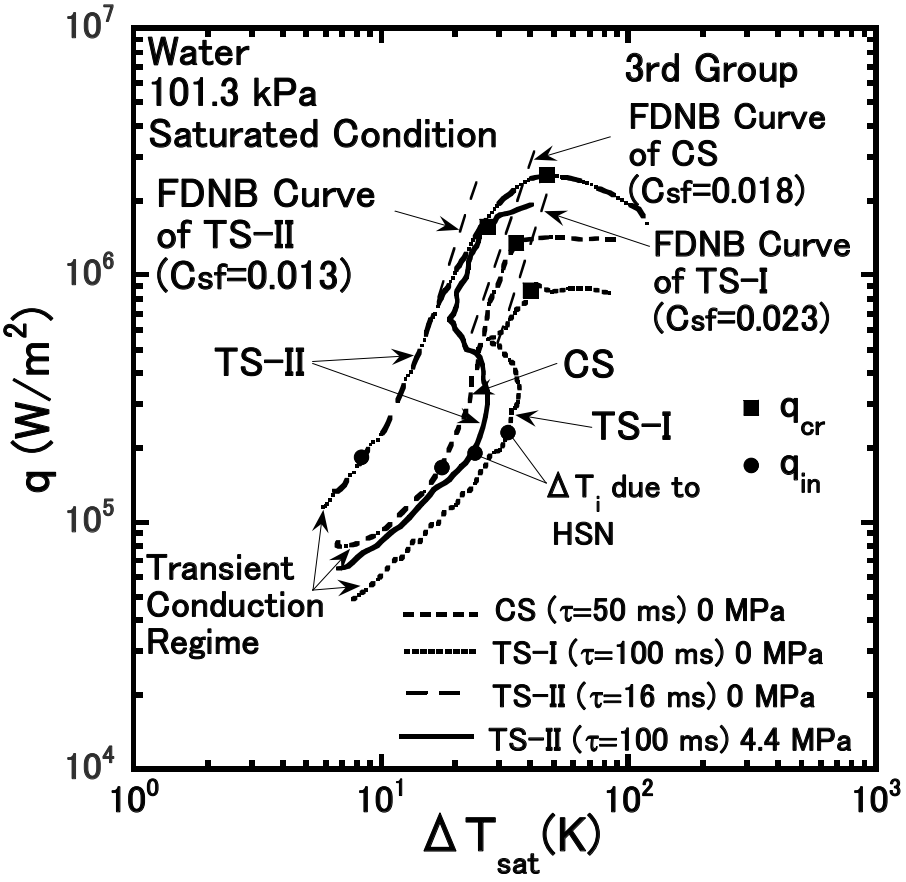

Fig.9 Typical heat transfer processes from transient conduction to film boiling with insufficient FDNB

lead to film boiling regime with a degradation of heat transfer and increasing of surface superheats, ΔT_{sat}. These kinds of heat transfer processes are usually occurred at the short period or τ <50 ms.

The heat transfer processes due to exponential period, τ , of 100 ms for TS-I (0 MPa) and TS-II (4.4 MPa), 50 ms for CS (0 MPa) and 16 ms for TS-II (0 MPa) are shown in Fig. 9. The heat transfer processes increase from transient conduction to film boiling with insufficient FDNB. The boiling initiations begin on conduction regimes, respectively. The values of ΔT_i for the CS (0 MPa), the TS-I (0 MPa), the TS-II (0 MPa) and the TS-II (4.4 MPa) are found at 17 K, 33 K, 9 K and 24 K, respectively, depending on the surface condition. The ΔT_i for the TS-I (0 MPa) is higher than the ΔT_i due to HSN attained on the TS-II (4.4 MPa). After boiling initiations, the ΔT_{sat} of the q of the TS-I (0 MPa) and the TS-II (4.4 MPa) first increase, then decrease and again increase with the increases of the heat fluxes, respectively. The explosive boiling with simultaneous HSN at the boiling initiations of the TS-I (0 MPa) and the TS-II (4.4 MPa) can degrade the heat transfer and increase the ΔT_{sat}. Then, the rapid activations of the cavities due to HSN decrease the surface superheats. The heat transfer processes do not reach to the respective FDNB regimes which are demonstrated by the broken lines in Fig.9. In case of TS-II (0 MPa) for period, τ , of 16 ms, it has a better heat transfer and higher CHF because the ΔT_i is due to active cavities and it was not affected by HSN. The higher to lower value of the CHF on the surface condition is attained on the order of TS-II, CS and TS-I, respectively. Because the ΔT_{sat} at the CHF and the ΔT_i due to HSN are similar for the TS-II (4.4 MPa) and the TS-I (0 MPa) as is seen in Fig.9, it is assumed that the CHFs achieved on the TS-II (4.4 MPa) and the TS-I (0 MPa) are resulting from the HSN. These kinds of heat transfer processes can be mainly observed at the intermediate period or 50 ms < τ <100 ms for the CS (0 MPa), the TS-I (0 MPa) and the TS-II (4.4 MPa), respectively, and 16 ms < τ <50 ms for the TS-II (0 MPa).

3.6 Transient CHF for CS, TS-I and TS-II

Figure 10 shows the transient CHF, q_{cr}, versus the exponential periods, τ, that were measured at atmospheric pressure under saturated conditions for CS (0 MPa), TS-I (0 MPa) and TS-II (0/4.4 MPa). The value of τ is ranging from 5 ms to 20 s. The values of CHF, q_{cr}, for the CS (0 MPa), the TS-I (0 MPa) and the TS-II (4.4 MPa) are in line with the typical trend according to the [5,6]: at first, it slightly increases up to maximum CHF from a steady-state CHF, then decreases down to minimum CHF and finally increases again with a decrease in period.

The first group of CHFs was resulted from the heat transfer processes as shown in Fig.7 and they were mainly observed at τ > 50 ms for the TS-II (0 MPa), τ >100 ms for the CS (0 MPa) and the TS-II (4.4 MPa), and τ > 200 ms for the TS-I (0 MPa), respectively. The CHFs for period measured on the TS-II (0/4.4 MPa) have the same value at the first group of CHF. However, it would seem that the experimental results of the TS-II (0 MPa) for τ ranging from 20 s down to 16 ms meet to the first group of CHF as is seen in Fig.10. However, when the heat transfer process of the TS-II (0 MPa) due to period, τ, of 16 ms was confirmed, it increased from transient conduction to film boiling without reaching the FDNB as shown in Fig.9. On the contrary, the heat transfer process of the TS-II (0 MPa) due to the period, τ, of 100 ms reaches to film boiling through the FDNB. Having consideration to these facts, the CHF resulting from the heat transfer processes due to τ ranging from 20 s down to 50 ms are considered to be the first group of CHF. At the measured first group of CHF for period, the TS-II (0/4.4 MPa) contribute the higher CHF of about 1.2 times and 1.5 times when compared with the CS (0 MPa) and the TS-I (0 MPa), respectively.

The first groups of CHFs were tested with the previous corresponding values as shown in Eq. (11) suggested by [5, 6] which is based on hydrodynamic instability model [3, 4], plotted with the solid lines. The Eq. (11) is the relation of quasi-steady-state CHF at subcooling, $q_{cst,sub}$, and period, τ. In this study, zero-subcooling is considered for the saturated condition.

$$q_{cr} = q_{cst,sub}(1 + 0.21\tau^{-0.5}) \quad (11)$$

$$q_{cr} = h_c(\Delta T_i(\tau) + \Delta T_{sub}) \quad (12)$$

$$h_c = (k_l \rho_l c_{pl}/\tau)^{1/2}, \text{ when } (t/\tau \geq 3) \quad (13)$$

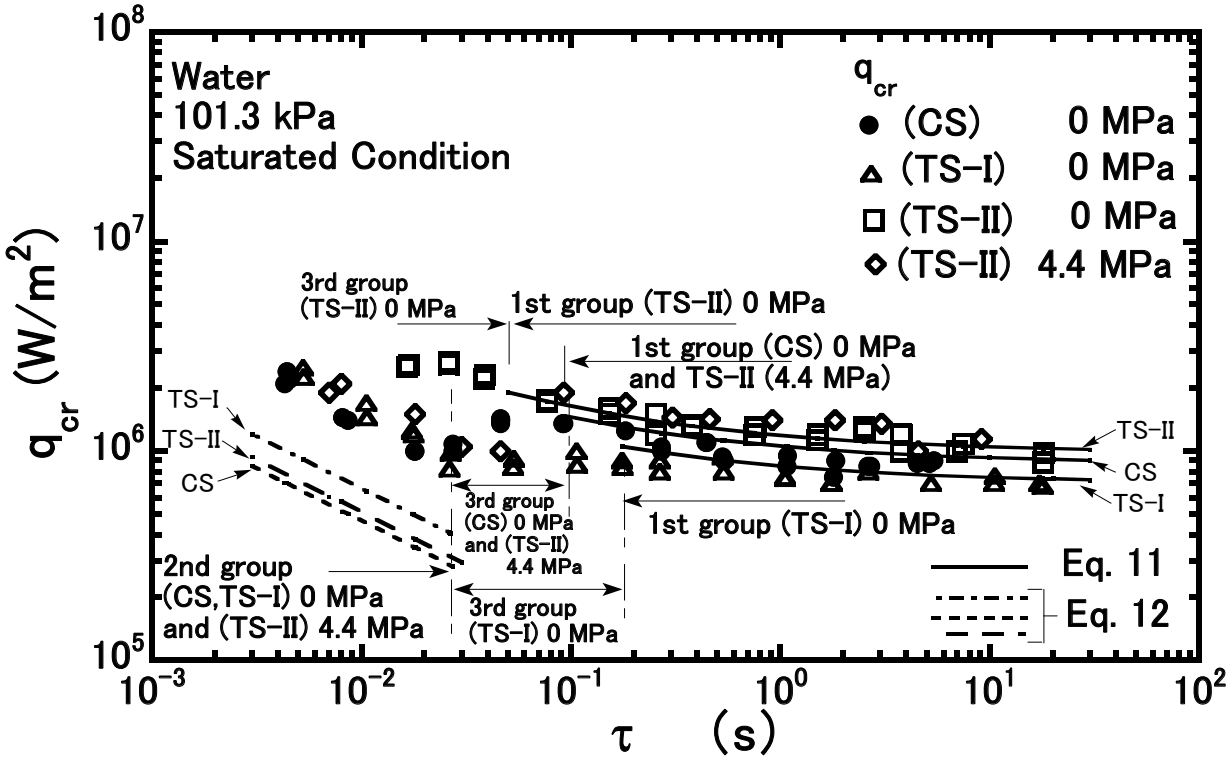

Fig. 10 Transient CHF for saturated conditions at atmospheric pressure with different surfaces

The second group of CHFs was occurred at the periods shorter than the periods corresponding to minimum CHFs which is shown in Fig.10. The second groups of CHFs attained only for the CS (0 MPa), the TS-I (0 MPa) and the TS-II (4.4 MPa) were induced by the semi-direct transition process that belongs to the typical heat transfer process as shown in Fig.8. The trend of the second groups of CHFs for the CS (0 MPa), the TS-I (0 MPa) and TS-II (4.4 MPa) are similar and increase asymptotically. However, a quite higher trend is observed on the TS-II (4.4 MPa).

They were evaluated by the previous CHF data as described by Eq. (12) [5,6] which compromised with the heat flux at boiling initiation for certain condition or direct transition to film boiling. The Eq. (12) is based on the conduction heat transfer coefficient, h_c , for exponential heat input, experimental surface superheat at boiling initiation due to HSN in transient conduction regime, ΔT_i , and the liquid subcooling, ΔT_{sub}. The value of h_c which is indicated in Eq. (13) has the equivalent function of $(k_l \rho_l c_{pl}/\tau)^{1/2}$ at the condition of $(t/\tau \geq 3)$ [27]. In this study, the heat transfer coefficient versus $t/\tau > 3$ for period, τ , of 20 ms can be seen in Fig.6. As depicted in Fig.10, the correlation does not correspond to the measured second group of CHF. It is caused by the facts that the occurrence of nucleate boiling for a while gives to an increase of the heat flux. In this study, as the ΔT_i of the TS-I (0 MPa) is higher than the others, the corresponding value according to the Eq. (12) for TS-I (0 MPa) which is illustrated by chain-line is higher than the other ones.

The third group of CHFs for period was induced by the heat transfer processes due to insufficient FDNB which belongs to the experiment results of the CS (0 MPa), the TS-I (0 MPa), the TS-II (0 MPa) and the TS-II (4.4 MPa) as shown in Fig.9. It was usually occurred on the region from the maximum CHF of the first group down to the minimum one of the second group. However, that of the TS-II (0 MPa) was found at the short period. The third group of CHFs for period due to the TS-I (0 MPa) is longer than the CS (0 MPa) and the TS-II (4.4 MPa). The third group of CHFs for period from higher trend to lower one are on the order of the TS-II (0 MPa), the TS-II (4.4 MPa), the CS (0 MPa) and the TS-I (0 MPa), respectively.

4. Conclusions

The experimental study on transient boiling heat transfer and critical heat flux on horizontal vertically oriented ribbons having different surfaces with CS, TS-I and TS-II in pool of water were carried out under saturated conditions at 101.3 kPa. The TS-II was subjected to the conditions without pre-pressurization and with pre-pressurization up to 4.4 MPa before each experimental run.

(1) The relation of the measured surface roughness and contact angle on CS, TS-I and TS-II agree with the previous corresponding relation based on the surfaces of copper and stainless steel.

(2) By pre-pressurization, the ΔT_i due to HSN which is depending on surface condition can be induced at boiling initiation even for quasi-steadily increasing heat input. The ΔT_i due to HSN does not affect to the CHF at the longer period. However, it affects to the CHF at the short exponential periods and the heat transfer process can lead to film boiling without a nucleate boiling.

(3) The heat transfer processes of TS-II (4.4 MPa) have the same transitions with the TS-I (0 MPa) and the CS (0 MPa) in short and intermediate exponential periods.

(4) For the same heat flux at each nucleate boiling regime, the TS-II (0/4.4 MPa) enhance the heat transfer ~290% and ~430 % relative to the CS (0 MPa) and the TS-I (0 MPa) by calculating with the Eqs. (6) and (8).

(5) The transient CHF, q_{cr} , on the shorter periods are higher than the longer ones because the heat transfer process of the short period at the non-boiling regime is influenced by the transient conduction and it can generate the higher value of CHF.

(6) Based on the measured first group of CHF for period, TS-II (0/4.4 MPa) contributes the higher CHF of about 1.2 times and 1.5 times when compared with those of CS (0 MPa) and TS-I (0 MPa), respectively.

(7) Transient CHFs, q_{cr} , for short periods on the CS (0 MPa), the TS-I (0 MPa) and the TS-II (4.4 MPa) are higher than the corresponding values.

Acknowledgements

Min Han Htet describes the gratitude to Graduate School of Maritime Sciences, Kobe University for financial supports throughout his study. The authors also appreciate to Ms. Rie SAKAMOTO and Mr. Hiroki MORISHITA for their vigorous cooperation at the Thermal Engineering Laboratory, Kobe University.

References

[1] I. A. Mudawwar, T. A. Incropera, and F. P. Incropera, Int. J. Heat Mass Transfer, 30, (1987-10), 2083-2095.
[2] K. Fukuda, Q. Liu, H. Kida, and, J. Park, Journal of JIME, 39, (2004), 33-41.
[3] S.S. Kutateladze, Heat transfer in condensation and boiling, AEC-tr-3770, USAEC (1959).
[4] N. Zuber, Hydrodynamic Aspects of Boiling Heat Transfer, AECU-4439, USAEC (1959).
[5] A. Sakurai, Nuclear Engineering and Design, 197, (2000), 301-356.
[6] K. Fukuda, M. Shiotsu, and A. Sakurai, Nuclear Engineering and Design, 200, (2000), 55-68.
[7] A. E. Bergles, Int. J. Refrig., 20, (1997-8), 545-551.
[8] H. O. Hanley, C. Coyle, J. Buongiorno, T. McKrell, L-W. Hu, M. Rubner, and R. Cohen, The 15th International Topical Meeting on Nuclear Reactor Thermal Hydraulics, Nureth-15, Pisa, Italy, May 12-17, (2013).
[9] P. Griffith, and J. D. Wallis, Heat Transfer-STORRS, Chemical Engineering Progress Symposium Series, 30, (1960-56), 49-63.
[10] C. Corty, and A. S. Foust, Chemical Engineering Progress Symposium Series, 51, (1955-17), 1-12a.
[11] P. J. Berenson, Int. J. Heat Mass Transfer, 5, (1962), 985-999.
[12] I. Golobič, and K. Ferjančič., Heat and Mass Transfer, 36, (2000), 525-531.
[13] J. M. Ramilison, P. Sadasivan, and J. H. Lienhard, Journal of Heat Transfer, 114, (1992), 297 -290.
[14] R.E. Faw, R.J. Vanvleet, and D.L. Schmidt, Int. J. of Heat and Mass Transfer, 29, (1986-9),1427-1437.
[15] B. Bon, C-K. Guan, and J. F. Klausner, Experimental Thermal and Fluid Science, 35, (2011-5), 746-752.
[16] A. Howard, and I. Mudawar, Int. J. Heat Mass Transfer, 42, (1999), 1665-1688.
[17] T. Harada, H. Nagakura, and T. Okawa, J. Engineering for Gas Turbines and Power, 132, (2010), 3949-3955.
[18] S. G. Kandlikar, and M. E. Steinke, Int. J. Heat Mass Transfer, 45, (2002), 3771-3780.
[19] Y. Honjo, M. Furuya, T. Takamasa, and K. Okamoto, Journal of Power and Energy System, 3, (2009-1), 216-227.
[20] S. G. Kandlikar, and M. E. Steinke, Trans IChemE, 79, Part A, (2001), 491-498.
[21] F. Raymond, The Platinum Metals and Their Alloys, (1941), 20.
[22] A. Sakurai, and M. Shiotsu, Journal of Heat Transfer, Trans. ASME, 99, (1977- Series C), 547-553.
[23] A. Sakurai, K. Mizukami, and M. Shiotsu, Heat Transfer 1970, Vol.V, B3.4, Elsevier, Amsterdam, (1970).
[24] T. Fujii, and M. Fujii, Int. J. of Heat and Mass Transfer, 19, (1976), 121-122.
[25] W.M. Rohsenow, Trans. ASME, 74, (1952), 969.
[26] A. Sakurai, M. Shiotsu, and K. Hata, Trans. ASME, 112, (1990), 441-450.
[27] S. Hayashi, A. Sakurai, and T. Iwazumi, The Engineering Research Institute, Kyoto University, 8, (1963-6), Report No.105.

Nomenclature

c_p	specific heat at constant pressure [J/kgK]
C_{sf}	values of liquid-solid combination
g	acceleration of gravity [m/s^2]
h_c	conduction heat transfer coefficient [W/m^{2}K]
h_{1v}	latent heat of vaporization [J/kg]
k	thermal conductivity [W/mK]
Pr	Prandtl number
Q_0	initial heat generation rate [W/m^3]
q_i	heat flux at boiling initiation [W/m^2]
q_{nb}	heat flux at nucleate boiling [W/m^2]
t	time [s]
x	coordinate along the thickness of the ribbon [m]
σ	surface tension [N/m]
ρ	density [kg/m^3]
μ	viscosity [Ns/m^2]

Subscripts

h	heater
l	liquid
v	vapor